



Published in final edited form as:

Stem Cells. 2015 June ; 33(6): 1850–1862. doi:10.1002/stem.1995.

Heparanase Released From Mesenchymal Stem Cells Activates Integrin beta1/HIF-2alpha/Flk-1 Signaling and Promotes Endothelial Cell Migration and Angiogenesis

Xinyang Hu^{#a,b}, Ling Zhang^{#a,b}, Jing Jin^{a,b}, Wei Zhu^{a,b}, Yinchuan Xu^{a,b}, Yan Wu^{a,b}, Yingchao Wang^{a,b}, Han Chen^{a,b}, Keith A. Webster^c, Huiqiang Chen^{a,b}, Hong Yu^{a,b}, and Jian'an Wang^{a,b}

^aDepartment of Cardiology, Second Affiliated Hospital, College of Medicine, Zhejiang University, Hangzhou, People's Republic of China

^bCardiovascular Key Laboratory of Zhejiang Province, Hangzhou, People's Republic of China

^cDepartment of Molecular and Cellular Pharmacology, Leonard M. Miller School of Medicine, University of Miami, Miami, Florida, USA

These authors contributed equally to this work.

Abstract

Heparanase plays important roles in tumor angiogenesis. Our previous study demonstrated that hypoxic preconditioning (HPC) enhanced the angiogenic and therapeutic effects of mesenchymal stem cells (MSCs), effects that were paralleled by enhanced heparanase expression. This study was designed to elucidate the role of heparanase in the improved therapeutic properties of HPC-MSCs and to explore underlying mechanisms using an ischemic rat hind limb model. MSCs transfected with heparanase (MSC^{hpa}) or empty vector (MSC^{null}) were delivered by intramuscular injections to ischemic hind limbs. Hind limbs that received MSC^{hpa} recovered blood flow more rapidly at 7 days and acquired higher capillary density at 14 days compared with MSC^{null}. Conditioned medium from MSC^{hpa} increased endothelial cell migration and promoted greater tube formation relative to that from the MSC^{null} groups. Vascular endothelial growth factor receptor 2 (VEGFR2, Flk-1) and its downstream signaling pathway (p38MAPK/HSP27) were significantly

This is an open access article under the terms of the Creative Commons Attribution-NonCommercial-NoDerivs License, which permits use and distribution in any medium, provided the original work is properly cited, the use is non-commercial and no modifications or adaptations are made.

Correspondence: Jian'an Wang, M.D., Department of Cardiology, Second Affiliated Hospital, College of Medicine, Zhejiang University, Cardiovascular Key Lab of Zhejiang Province, Hangzhou 310009, People's Republic of China. Telephone: 86-571-87783992; Fax: 86-571-87037885; jian_an_wang@yahoo.com or Xinyang Hu, M.D., Department of Cardiology, Second Affiliated Hospital, College of Medicine, Zhejiang University, Cardiovascular Key Lab of Zhejiang Province, Hangzhou 310009, People's Republic of China. Telephone: 86-571-87783992; Fax: 86-571-87037885; hxy0507@126.com.

Author Contributions

X.H.: conception and design, data analysis and interpretation, manuscript writing, and final approval of manuscript; L.Z.: conception and design, collection and/or assembly of data, and manuscript writing; J.J., Y.Wu, Y.Wang, Han Chen, and Huiqiang Chen: collection and/or assembly of data; W.Z.: conception and design, data analysis and interpretation, and manuscript writing; Y.X.: data analysis and interpretation; K.A.W.: data analysis and interpretation and manuscript preparation; H.Y.: data interpretation and manuscript preparation; J.W.: conception and design, financial support, provision of study material or patients, and final approval of manuscript. X.H. and L.Z. contributed equally to this article.

DISCLOSURE OF POTENTIAL CONFLICTS OF INTEREST

The authors indicate no potential conflicts of interest.

increased in human umbilical vein endothelial cells (HUVECs) after treatment with MSC^{hpa} conditioned medium. Each of these responses was decreased by cocultured with MSC^{hpa}-KD conditioned medium. MSC^{hpa} conditioned medium activated hypoxia-inducible factor-2 α (HIF-2 α) and increased in parallel the transcript level of Flk-1 as determined by chromatin immunoprecipitation-PCR and luciferase assays. Analyses of integrin expression revealed an important role for integrin β 1 in the regulation of HIF-2 α . All angiogenic effects of MSC^{hpa} conditioned medium were abolished by knockdown of integrin β 1, HIF-2 α , and Flk-1 in HUVECs with selective shRNAs. These findings identify heparanase as a key regulator of angiogenesis by MSCs. We propose a novel pathway wherein heparanase sequentially activates integrin β 1, HIF-2 α , Flk-1, and p38MAPK/HSP27 with corresponding enhancement of angiogenesis.

Keywords

Heparanase; Angiogenesis; Mesenchymal stem cell

Introduction

Occlusive vascular disease is a major cause of morbidity and mortality. Treatment possibilities for the two major cardiovascular consequences, myocardial infarction, and peripheral artery disease (PAD) are often limited to palliative interventions such as angioplasty and bypass surgery [1]. For clinical limb ischemia, the end-stage of PAD, amputation may be the only option for many patients. Therapeutic angiogenesis, by gene or cell therapy to stimulate collateral formation, has emerged as a novel approach for treating occlusive vascular diseases [2]. For cell therapy, bone marrow mesenchymal stem cells (MSCs) are considered a promising option because of their unique biological attributes including immunosuppression, self-renewal, and multipotent differentiation abilities [3]. Both animal studies and clinical trials have recently confirmed that MSC transplantation stimulates angiogenesis and blood flow recovery in ischemic muscle [4]. Autologous therapy with MSCs may be limited by the age and clinical condition of the donor that influence cell function [5]. Allogeneic MSC therapy may overcome this limitation, but still suffers from poor cell survival after transplantation that restricts the biological activities and therapy. New approaches and techniques are needed to further enhance the biological and therapeutic activities of allogeneic MSCs.

Heparanase (HPA), an endo- β -glucuronidase, has been shown to contribute to cell dissemination during tumor metastasis and activation of angiogenesis. It cleaves heparin sulfate side chains, causing extracellular matrix remodeling and release of heparan sulfate-bound molecules including growth factors and inflammatory cytokines [6]. HPA enzyme has been shown to be associated with breakdown of the basement membrane and may facilitate inflammatory cell migration and invasion by exposing cell adhesion sites on the vascular endothelium [7]. HPA is also involved in regulating cell signaling and gene transcription [8, 9]. For example, HPA induces endothelial cell migration via protein kinase B/Akt activation [10] and VEGF expression via Src signaling [11].

Previously we found that hypoxic preconditioning (HPC) significantly enhanced the angiogenic potential of MSC therapy [12] and HPA expression was elevated in parallel (Supporting Information Fig. S1). However, it is unknown whether HPA has a role in the HPC enhanced therapeutic effects of MSCs. Therefore, in this study, we used gain and loss of HPA function in MSCs to investigate the potential therapeutic roles of HPA in a rat ischemic hind limb model. We found that HPA overexpression in MSCs conferred significantly augmented angiogenesis and cell invasion through a novel pathway that was mediated by integrin $\beta 1$ /hypoxia-inducible factor-2 α (HIF-2 α) and Flk-1.

Materials and Methods

Cell Culture

Primary human umbilical vein endothelial cells (HUVECs) were a gift from Dr. Yi Wang (Zhejiang University, Zhejiang, China). HUVECs, at passages between 4 and 8, were cultured in gelatin-coated flasks in Dulbecco's modified Eagle's medium (DMEM) (Gibco, Grand Island, NY) supplemented with 20% Fetal bovine serum (FBS, Corning, Brisbane, Australia), 50 U/ml heparin (Shanghai No. 1 Biochemical Pharmaceutical Co, Shanghai, China), and 100 U/ml penicillin (Zhongguo Pharmaceutical (shijiazhuang) Co, shijiazhuang, China) plus 100 mg/ml streptomycin (Northern China Pharmaceutical Co, shijiazhuang, China) (pen/strep). MSCs were harvested from femurs and tibias of male Sprague-Dawley (SD) rats as described previously [13] and cultured with DMEM/20% FBS and pen/strep to passages 3–8. The immunophenotype of MSCs from rats was assessed by flow cytometry using specific cell surface antigens. The cells expressed the MSCs markers CD29, CD44, CD73, CD90, and CD105 and were negative for the markers CD31, CD34, and CD45 [14].

Animal and Experimental Protocol

Male SD rats (250 g) were purchased from Zhejiang Experimental Animal Center. Animals were fed a standard laboratory diet with free access to food and water, kept in a controlled room temperature ($22^{\circ}\text{C} \pm 1^{\circ}\text{C}$), humidity (65%–70%), and a 12:12 hours light/dark cycle. All procedures were approved by the Animal Ethic Review Committee of Zhejiang University and are in compliance with NIH Publication No. 85-23 (revised 1996). Surgical procedure to induce limb ischemia was exactly as previously described [15]. After operation, rats were divided into the following groups: Control group (CON, phosphate buffer saline, PBS treatment), MSC group (MSC, MSC treatment), and HPA overexpression MSC group (MSC^{hpa}, MSC^{hpa} treatment).

Cell Preparation and Transplantation

MSCs were transduced with Lenti-Null, or Lenti-HPA as described by the manufacturer (Genechem Company, Shanghai, China). Immediately after femoral artery ligation, 2×10^5 cells (50 μl in PBS) were injected into the quadriceps femoris muscle of the rat right hind limb. PBS injection was also used as negative control.

Laser-Doppler Imaging

Blood flow was measured using laser Doppler imaging (LDI) (MLDI 5063, Moor Instruments, Ltd., Devon, U.K.) as described [16]. LDI measurements were performed

before occlusion, immediately after, then at 3, 7, and 14 days post-surgery. The right-to-left (*R/L*) ratio (operated vs. nonoperated leg) was calculated for each animal ($n = 7$ for each group).

Condition Medium Collection

MSCs were seeded at a density of 1×10^5 cells in six-well plates, cultured for 24 hours, and the medium replaced with 2 ml of DMEM plus 10% FBS for additional 48 hours, conditioned medium was centrifuged (2,500 rpm for 3 minutes) to remove cell debris and used for experiments.

Migration Assay

HUVEC migration was performed in a Transwell chemotaxis 24-well chamber (Corning Glassworks, Corning, NY, USA) as described previously [17]. In brief, 2×10^4 cells/well were plated in the upper chamber of in DMEM with 1% FBS. The lower chamber was filled with MSC-conditioned medium or control medium as above or with recombinant human active heparanase (100 mg/ml, R&D Systems, Minneapolis, MN, USA). After 6 hours at 37°C, nonmigrating cells were removed from the filter by washing three times with PBS and gentle scraping. Migrated cells present on the lower aspect of the filter were fixed with 10% formaldehyde for 30 minutes and stained with 0.1% crystal violet for 20 minutes. Five fields were counted for each well (original magnification, $\times 200$). Migrated cells were quantified by Image-Pro Plus 6.0 (Media Cybernetics, Bethesda, MD, USA).

Tube Formation of HUVECs

A Matrigel tube-formation assay was performed to assess in vitro angiogenesis [18]. HUVECs plated at 2×10^4 cells/well were incubated with conditioned medium or recombinant heparanase (100 mg/ml) in 96-well plates precoated with growth factor-reduced Matrigel (BD, San Jose, CA, USA). After 4–6 hours, five fields were counted for each well (original magnification, $\times 100$). The mean tube length was quantified by Image-Pro Plus 6.0.

Immunohistochemical Staining

Tissues were rapidly excised and fixed in neutral buffered formalin, embedded in paraffin, and 5 μ m sections were stained with H&E. Immunohistochemistry was performed to determine capillaries and small arteries using primary antibodies as follows: rabbit anti-CD31 (Chemicon, Temecula, CA, USA) and α -smooth muscle actin (α -SMA, Eptomics; Burlingame, CA, USA), then incubated with respective secondary antibodies and nuclei were counterstained with 4',6-diamidino-2-phenylindole (DAPI, Vector Laboratories, Burlingame, CA, USA). The number of positive staining of each section was counted in five different fields (original magnification, $\times 400$).

Chromatin Immunoprecipitation-PCR

Chromatin immunoprecipitation (ChIP) assays were performed as described previously [19]. Briefly, HUVECs (5×10^7 cells) were incubated with recombinant HPA (100 mg/ml) and cross-linked with 1% formaldehyde for 10 minutes at 37°C. Cross-linking was stopped by the addition of 0.125 M glycine. The cells were washed three times with ice-cold PBS and

kept on ice for 10 minutes in 25 mM HEPES (pH 7.8), 1.5 mM MgCl₂, 10 mM KCl, 0.1% Nonidet P40, 1 mM dithiothreitol, 0.5 mM phenylmethylsulfonyl fluoride, and protease inhibitor mixture (Roche, Base, Switzerland). Nuclei were collected and sonicated on ice to shear DNA to an average length of 200 bp. After sonication, the chromatin solution (500 µg) was incubated with ChIP grade antibodies against HIF-2 α (Abcam, Cambridge, MA, USA) or rabbit normal IgG (Abcam, Cambridge, MA, USA) at 4°C overnight. Antibody-bound complexes were obtained, and DNA fragments extricated from these complexes were purified using a QIAquick PCR purification kit (Qiagen, Duesseldorf, Germany). The purified ChIPed DNA samples were analyzed by conventional PCR using specific forward and reverse FLK1 promoter primers (Supporting Information Table S1).

Luciferase Reporter Assay

Plasmids containing KDR and the pCDNA3.0-HIF-2 α promoter and control plasmid pCDNA3.0 were constructed by Genechem Company and Shanghai Newgene Biosciences Company. 293T cells were maintained in DMEM with 10% FBS. Roche X-tremeGENE HP DNA Transfection Reagent was used for transfection. 1.2×10^5 293T cells per well in 96-well plates were transfected with a mixture including 1 µg plasmid, 100 µl of serum-free DMEM, and 6 µl of Roche X-tremeGENE HP DNA Transfection Reagent. The Dual-Glo Luciferase Assay (Promega, Madison, WI, USA) was performed at 48 hours after transfection and luminescence was measured using SpectraMax M5 (Molecular Devices, Sunnyvale, CA, USA). Data are presented as the means SD of triplicate well measurements for one representative experiment.

Western Blotting

Cells were rinsed with cold PBS, lysed in 2.5× SDS gel loading buffer (30 mM Tris-HCl [pH 6.8], 1% SDS, 0.05% bromophenol blue, 12.5% glycerol, and 2.5% mercaptoethanol) and then boiled for 30 minutes. Equal amounts of cell lysates were resolved on 10% or 12% SDS polyacrylamide gels, and the proteins electro-transferred to polyvinylidene fluoride (PVDF) membranes (Millipore, Boston, MA, USA). The blots were incubated with the indicated primary antibodies, HPA (1:1,000, Cell Signaling Technology, Danvers, MA, USA), HIF-2 α (1:200, Abcam, Cambridge, MA, USA), Flk-1 (1:200, Santa cruz biotechnology, Dallas, Texas, USA), P-p38 (1:1,000, Cell Signaling Technology, Danvers, MA, USA), p38 (1:1,000, Cell Signaling Technology, Danvers, MA, USA), P-hsp27 (1:1,000, Cell Signaling Technology, Danvers, MA, USA), hsp27 (1:1,000, R&D Systems, Minneapolis, MN, USA), Ang1 (1:1,000, Abcam, Cambridge, MA, USA), Tie2 (1:1,000, Abcam, Cambridge, MA, USA), P-NF-KBp105 (1:500, Signalway Antibody, College Park, Maryland, USA), NF-KBp105 (1:1,000, Cell Signaling Technology, Danvers, MA, USA), P-NF-KBp50 (1:500, Signalway Antibody, College Park, Maryland, USA), NF-KBp50 (1:1,000, Cell Signaling Technology, Danvers, MA, USA), P-NF-KBp65 (1:1,000, Abcam, Cambridge, MA, USA), NF-KBp65 (1:1,000, Abcam, Cambridge, MA, USA), HIF-1 α (1:500, Signalway Antibody, College Park, Maryland, USA), Flt-1 (1:500, Proteintech, Chicago, IL, USA), VEGF (1:1,000, Abcam, Cambridge, MA, USA), P-ERK (1:1,000, Cell Signaling Technology, Danvers, MA, USA), ERK (1:1,000, Cell Signaling Technology, Danvers, MA, USA), P-AKT (1:1,000, Cell Signaling Technology, Danvers, MA, USA), AKT (1:1,000, Cell Signaling Technology, Danvers, MA, USA), actin (1:3,000,

KANGCHEN, shanghai, China), followed by horseradish peroxidase-conjugated secondary antibodies. Immunoreactivity was visualized using chemiluminescence ECL Western-blotting system (Millipore, Boston, MA, USA), Wild-type MSC (MSC^{WT}) and MSCs transduced with Lent-Null (MSC^{null}) were used as an essential controls.

Lentivirus Construction and Infection

Construction of the recombinant lentivirus with HPA, HIF-2 α , and Flk-1 was performed by Genechem Company. For MSCs or HUVECs cell infection, cells were seeded at a density of 1×10^5 cells in a six-well plate and infected with different lentiviral vectors in the presence of 10 μ g/ml polybrene (Millipore, Boston, MA, USA). At 12 hours postinfection, the growth medium was replaced. Forty-eight hours later, green fluorescent protein expression of transduced cells was observed under fluorescence microscopy and then the transfected cells were cultured in a 5% CO₂-humidified incubator at 37°C.

Aortic Ring Outgrowth Assays

Ex vivo aortic ring angiogenesis assays were carried out as previously described with the following condition modifications [20]. Thoracic aortas were isolated from 250 g SD rat, sectioned into 1 mm rings. Rings were cultured in growth factor-reduced Matrigel (BD, San Jose, CA, USA) polymerized at 37°C. Assay conditions included 300 μ l MSC-conditioned medium or control medium was refreshed every 3 days, and cultures maintained at 37°C in a humidified incubator under normoxia (21% O₂). Angiogenesis was assessed at day 7 using an inverted microscope platform (Leica DMI6000B, Biberach, Germany). Total vessel outgrowth was summed for each ring using image proplus 6.0 software ($n = 3$).

ELISA Assay

ELISA kits were used to quantify HPA (Blue gene), PDGF-BB (R&D Systems, Minneapolis, MN, USA), TGF- β (R&D Systems, Minneapolis, MN, USA), HGF (R&D Systems, Minneapolis, MN, USA), and VEGF (R&D Systems, Minneapolis, MN, USA). Conditioned medium was collected from MSC^{WT}, MSC^{hpa}, MSC^{null}, MSC^{hpa-KD}, and MSC^{hpa} with OGT2115 and analyzed according to the manufacturer's instructions.

Statistical Analysis

All data are presented as means \pm SD. Statistical analyses were performed by one-way ANOVA using the SPSS 17.0 software. Probability values of $p < .05$ were considered to be significant.

Results

Augmented Angiogenesis by HPA Over-Expressing MSC (MSC^{hpa})

Consistent with our previous study, we showed HPC-MSCs conferred improved blood flow in a rat hind limb ischemia model compared with normoxic MSCs, the augmented angiogenic effect of HPC was paralleled with enhanced HPA expression and was abolished by MSC^{hpa-KD}. CD31 and SMA immunostaining confirmed this effect (Supporting Information Fig. S1). These results suggest an important role for HPA in new vessel

formation and limb perfusion. To evaluate whether enhanced HPA expression of MSCs is sufficient to promote angiogenesis, we evaluated vascular regeneration in the rat model by transplanting syngeneic MSCs transfected with lentiviral HPA (MSC^{hpa}) or MSCs transfected with empty vector (MSC^{null}) as described in Materials and Methods. Over-expression of HPA in MSC^{hpa} was confirmed by Western blot and ELISA (Fig. 1C, 1D). From day 3 to day 14 after cell transplantation, blood flow in the ischemic hind limb increased only marginally in the MSC^{null}-treatment group compared with PBS controls ($p > .05$). In contrast, the MSC^{hpa}-treatment group showed significantly improved blood flow compared with either PBS or the MSC^{null}-treatment group ($p < .05$, respectively, Fig. 1A–1C). On day 14, immunostaining confirmed significantly increased CD31 and SMA positive vessels in the MSC^{hpa}-treatment group compared with either MSC^{null}-treated or PBS ($p < .01$, respectively) (Fig. 1E–1G). These results suggest an important role for MSC^{hpa} in new-vessel formation and improved limb perfusion.

To further characterize the proangiogenic properties of MSC^{hpa}, we used an aortic ring assay [20] and quantified angiogenic sprouting after exposure to conditioned media from MSC^{hpa}, MSC^{null}, and MSC^{hpa-KD} (HPA knockdown) as described in Materials and Methods. Knockdown of HPA in MSC^{hpa-KD} was confirmed by Western blot and ELISA (Fig. 2A, 2B). Consistent with our previous in vivo studies, conditioned medium from MSC^{hpa} resulted in longer sprouting length (SL, 256.6 ± 61.5) and a larger sprouting area (SA, 107661.0 ± 34330.5) as compared to MSC^{null} conditioned medium (SL, 126.1 ± 46.7 ; SA, 29060.4 ± 9062.3 . $p < .05$ and $p < .01$, respectively), while the proangiogenic effect was not observed in the MSC^{hpa-KD} group (Fig. 2E–2G). Next we used a matrigel HUVEC tube assay and compared conditioned media from MSC^{hpa}, MSC^{null}, and MSC^{hpa-KD} (HPA knockdown). As shown in Figure 2C, 2D, conditioned medium from MSC^{hpa} promoted HUVEC tube formation with longer capillary-like extensions and more complete vascular networks compared with MSC^{null} and the beneficial effects of MSC^{hpa} were lost in the MSC^{hpa-KD} group.

To further characterize the impact of HPA on angiogenesis, we compared the effects of conditioned medium from MSC^{hpa} or MSC^{null} on endothelial (HUVEC) migration using a transwell assay. As shown in Figure 3A, 3B, HUVEC migration was significantly augmented by conditioned medium from MSC^{hpa} compared with MSC^{null} and this effect was again attenuated by conditioned medium from MSC^{hpa-KD} (Fig. 3A, 3C). Together, these results confirm the proangiogenic properties of MSC^{hpa} and paracrine effects when cocultured with endothelial cells.

Enhanced Angiogenesis by MSC^{hpa} Conditioned Medium Is Mediated by Flk-1

One function of HPA is to cause the release of growth factors that are sequestered on heparin sulfate chains at the cell surface. To address the mechanism of MSC-HPA-mediated angiogenesis of HUVECs, we quantified the activities of key angiogenic cytokines, vascular endothelial growth factor (VEGF), and their receptors. Surprisingly, VEGF expression was unchanged in response to conditioned medium from MSC^{hpa} or MSC^{null} whereas VEGF receptor 2 (VEGFR2, Flk-1, and KDR), the receptor that mediates most of the known cellular responses to VEGF [21], was significantly increased in HUVECs after treatment

with MSC^{hpa} conditioned medium compared with MSC^{null} conditioned medium (Fig. 3D). Consistent with this, MSC^{hpa-KD} conditioned medium significantly decreased Flk-1 expression in HUVECs, resulting in an even lower level than that conferred by MSC^{null} (Fig. 3D). Moreover, these effects of HPA were specific for Flk-1 because related signaling factors intermediates including Flt-1, angiopoietin 1, and its receptor Tie 2 were not affected (Fig. 3D).

Cell migration is increased when VEGF binds Flk-1 and activates its downstream targets, p38MAPK/HSP27 [22, 23]. In this study, we confirm that enhanced Flk-1 expression in HUVECs induced by conditioned MSC^{hpa} medium was associated with increased phosphorylation of p38 and HSP27 compared with MSC^{null} conditioned medium, and the increased phosphorylation was abrogated when HUVECs were treated by MSC^{hpa-KD} conditioned medium (Fig. 3E). In contrast, phosphorylation of ERK and Akt did not correlate with HPA expression, suggesting that p38/HSP27 but not ERK or Akt pathways are implicated in MSC^{hpa} conditioned medium-induced angiogenesis (Fig. 3E).

To further elucidate the role of Flk-1 signaling in the enhanced angiogenesis by MSC^{hpa} conditioned medium, we implemented parallel HUVEC assays where the expression of Flk-1 was knocked down using Lenti-shRNA (see Materials and Methods). As shown in Figure 4A–4D, the enhanced migration and tube formation of HUVECs by MSC^{hpa} conditioned medium were eliminated by Flk-1 KD of recipient HUVECs. We further examined the effect of Flk-1 KD on p38/HSP27 phosphorylation levels. Protein levels of P-p38 and P-HSP27 were significantly decreased in Flk-1 KD HUVECs (Fig. 4E). Based on these results, we propose that HPA activates Flk-1 and this is a key component in the pathway of MSC^{hpa}-induced angiogenesis.

MSC^{hpa} Increases Flk-1 Expression Through Activation of HIF-2 α in HUVEC

While it is well established that Flk-1 is regulated precisely in a spatiotemporal manner during vascular development [24], the signaling intermediates for Flk-1 expression remain incompletely understood [25]. Previous work has shown that transcription factors HIF-2 α and NF- κ B are the two important angiogenic regulators [26]; therefore, we quantified HIF-2 α and NF- κ B activities in HUVECs that were exposed to the conditioned medium from MSC^{hpa} or MSC^{null}. As shown in Figure 5A, 5B, MSC^{hpa} conditioned medium increased total HIF-2 α protein and its nuclear accumulation compared with MSC^{null} conditioned medium treatment. In contrast, NF- κ B (p-p65, p-p50, and p-p105) was not changed by MSC^{hpa} conditioned medium (Fig. 5B). Moreover, HUVEC HIF-2 α expression was significantly depressed by treatment with conditioned medium from MSC^{hpa-KD} compared with MSC^{null} conditioned medium (Fig. 5B), whereas no changes were seen in NF- κ B (p-p65, p-p50, and p-p105) (Fig. 5B). Also, no changes were seen in HIF-1 α expression either treated with MSC^{hpa-KD} or MSC^{hpa} conditioned medium (Fig. 5B). These findings suggest that HIF-2 α is positively regulated by MSC^{hpa} conditioned medium.

To further investigate the role for HIF-2 α as the mediator of the effects of MSC^{hpa} on Flk-1 expression, we used lentishRNA to knockdown HIF-2 α in HUVECs (see Materials and Methods) and reanalyzed Flk-1 expression as well as migration and tube formation capability in HUVECs (Supporting Information Fig. S2A, S2B). As shown in Figure 5C–5E,

HUVEC migration was significantly reduced by HIF-2 α KD, and the enhanced migration and tube formation of HUVECs by MSC^{hpa} conditioned medium were eliminated by HIF-2 α KD of recipient HUVECs. Consistent with this phenotype, HIF-2 α KD significantly decreased Flk-1 expression in HUVECs. Furthermore, in HIF-2 α KD HUVECs, conditioned medium from MSC^{hpa} was no longer able to upregulate Flk-1 expression (Fig. 5F). Based on these results, we propose that MSC^{hpa} conditioned medium increases the cellular and nuclear accumulation translocation of HIF-2 α and this upregulates Flk-1 expression.

To further elucidate how HIF-2 α regulates Flk-1, ChIP-PCR and luciferase assays were performed. ChIP-PCR identified several binding sites for HIF-2 α on the Flk-1 gene promoter (Fig. 5G, 5H). The transcriptional response of Flk-1 to HIF-2 α was confirmed by luciferase reporter (Fig. 5I). These data suggest that HIF-2 α can directly regulate transcription of Flk-1 by promoter binding.

Possible Role for Integrin β 1 in the Activation HIF-2 α by MSC^{hpa}

Previous work has shown that HPA augments the expression integrin β 1 in brain, glioma cells, and metastatic breast cancer cells thereby enhancing angiogenesis [27, 28]. Because HPA did not increase VEGF expression in our studies we reasoned that an alternative pathway operated. Therefore, we examined integrin expression and found that multiple integrins including integrin β 1 were indeed upregulated by conditioned medium from MSC^{hpa}. In support of a role for HPA in this we found that integrin β 1 expression was decreased in HUVECs by treatment with conditioned medium from MSC^{hpa-KD} relative to that from MSC^{null} (Fig. 6A). To determine causative effects of this, we used lenti-shRNA to KD integrin β 1 in HUVECs and showed that the migration of integrin β 1-KD HUVECs was significantly decreased compared with HUVEC treated with vector controls (Fig. 6B, 6C). Furthermore, in integrin β 1-KD HUVECs, conditioned medium from MSC^{hpa} was no longer able to activate migration (Fig. 6C). This suggests a possible intermediate role for integrin β 1 in HPA-induced HUVEC migration. To further investigate the relationship between HIF-2 α activation and integrin β 1, we measured HIF-2 α expression in HUVECs while titrating integrin β 1 expression with interference shRNAs. Increased integrin β 1 was accompanied by activation of HIF-2 α , whereas integrin β 1 KD resulted in decreased HIF-2 α (Fig. 6B). This suggests that integrin β 1 may regulate HIF-2 α expression and hence mediate the effects of HPA (MSC^{hpa}) on angiogenesis.

HPA Is the Key Mediator of Angiogenesis in Conditioned Medium

As shown above, HPA levels were significantly increased in conditioned medium from MSC^{hpa} compared with that from MSC^{null} (Fig. 1D), while they were significantly decreased in MSC^{hpa-KD} conditioned medium (Fig. 2B), indicating that soluble HPA was present in the conditioned medium. Meanwhile, HGF was observed to be significantly changed either in conditioned medium of MSC^{hpa} or MSC^{hpa-KD} (Fig. 6E), but the concentration of VEGF, PDGF-BB, and TGF- β was not significantly different in different MSCs (Fig. 6D, 6E). To gain additional evidence that soluble HPA is a key angiogenic factor of conditioned medium, HPA inhibitor OGT2115 was used to selectively block HPA activity [29]. We found that 3.2 μ M OGT2115 blocked elevated HPA levels in conditioned medium without cytotoxicity (Fig. 6F, 6H) and significantly reduced the HUVEC migration (Fig. 6G,

Supporting Information Fig. S2C); however, the levels of VEGF, TGF- β , HGF, and PDGF-BB in the conditioned medium were unchanged (Fig. 6I).

To further confirm the effect of HPA, we added active recombinant human heparanase to HUVEC^{null} and HUVEC^{integrin β 1-KD} cultures to mimic the beneficial effect of HUVEC^{hpa}-conditioned medium. We found that active heparanase induced significant migration and tube formation and this was abolished in HUVEC^{integrin β 1-KD} cultures (Fig. 6J, 6K, Supporting Information Fig. S2D, S2E). In addition, active heparanase significantly increased integrin β 1, HIF-2 α , and Flk-1 expression in treated HUVECs (Fig. 6L).

Discussion

In this study, we describe a key role for HPA in the enhanced proangiogenic properties of MSCs. Our results support a pathway wherein HPA and/or a related secreted intermediate by MSCs acts on integrin β 1 receptors on endothelial cells (HUVECs) to promote the transcriptional activation of HIF-2 α , upregulation of Flk-1, and activation of Flk-1 downstream p38/HSP27 signaling (Fig. 7). Thus, our results underscore a novel signaling pathway of HPA and integrin β 1/Flk-1/HIF-2 α axis in enhanced endothelial cell migration and augmented angiogenesis.

Treatment with MSC^{hpa} marginally increased blood flow in the ischemic hind limb as compared to PBS group, it suggests an important role for HPA in MSC-induced angiogenesis. While MSC^{null} treatment did not observe significant improvement of blood flow, perhaps because the number of cell transplantation was less than previously reported [30]. HPA can activate angiogenesis by both enzymatic (heparin sulfate cleavage) and nonenzymatic pathways [31]. In the former, sequestered growth factors and cytokines are released from the extracellular matrix in active forms and target endothelial cells. Alternatively, the nonenzymatic pathways are independent of endoglycosidase activity [11]. In this study, we found that conditioned medium of MSC^{hpa}-induced migration and tube formation was associated with higher concentration of soluble HPA and HGF in the conditioned medium; however, VEGF, PDGF-BB, and TGF- β were not changed. HPA inhibitor OGT2115 inhibited the secretion of HPA and the migration of HUVEC, but did not reduce VEGF, HGF, TGF- β , or PDGF-BB levels. Furthermore, active heparanase treatment conferred the same beneficial effects as MSC^{hpa} conditioned medium. Therefore, we speculate that HPA is an important, although possibly not the sole mediator of conditioned medium and it exhibits both enzymatic and nonenzymatic functions. In this study, we paid particular attention to secreted HPA and we acknowledge that other angiogenic growth factors may be activated by HPA enzymatic activity.

Notably we found that Flk-1 was markedly upregulated in HUVECs by conditioned medium from HPA overexpressing MSCs, and this was attenuated by HPA KD. We further confirmed that these angiogenic readouts were Flk-1-dependent because they were eliminated by KD of Flk-1 in receptive HUVECs (Fig. 4A–4D). These findings strongly suggest that Flk-1 is essential for the enhanced angiogenesis mediated by MSC^{hpa}. Thus, our data support the widely acknowledged notion that Flk-1 is the key angiogenic mediator of VEGF [32–34]. Expression of Flk-1 acquired by embryonic stem cells confers differentiation into

endothelial cells [32]. Flk-1 positive neural stem cells have the potential to give rise to vascular endothelial cells [33]. Flk-1 can also regulate angiogenesis via a VEGF-independent manner [34].

In addition to Flk-1, phosphorylation of p38 and HSP27 was increased by MSC^{hpa} medium and this was abrogated by MSC^{hpa-KD} medium. In Flk-1 KD HUVECs, protein levels of P-p38 and P-HSP27 were also significantly decreased. This data suggest that HPA secreted by MSCs exerts paracrine effect that mediates HUVEC migration and angiogenesis in a Flk-1-dependent manner driven by activated p38 (MAPK) and HSP27 as the downward targets.

Flk-1 expression is regulated by hypoxia-inducible factors (HIF) [35]. While HIF-2 α is partially endothelial cell specific [36]. It has been reported that HIF-2 α , but not HIF-1 α , cooperates with Ets-1 in activating transcription of Flk-1 [37]. A tandem HIF-2 α binding site is identified within the Flk-1 promoter that acts as a strong enhancer element [37]. In our study, we found that HPA activated HIF-2 α , and this was closely associated with Flk-1 expression. Flk-1 regulation by HIF-2 α was also supported by our Chip and luciferase studies. An essential role for HIF-2 α in this pathway was also confirmed by gain and loss of function assay (Fig. 5D, 5E).

Our results further suggested that HIF-2 α activation is regulated by integrin β 1 downstream of HPA. Previous work has shown that HIF-2 α is regulated by hypoxia, environmental stimuli, Sp1/Sp3, and PAR-2 [38, 39]. PAR-2 enhances HIF-2 α expression through an integrin-linked kinase pathway that includes integrin β 1 [39]. We found that integrin β 1 was induced by HPA coincident with upregulated HIF-2 α , while knockdown of integrin β 1 resulted in HIF-2 α downregulation (Fig. 6B). The integrin β 1 gene may indeed be directly activated by hypoxia (HPC) through HIF-1 DNA binding sites in the promoter [40]. Our observation that HPA can activate integrin β 1 is also consistent with previous work showing augmented integrin β 1 expression by HPA in brain metastatic breast cancer cells [27] and human glioma cells, the latter coincident with induced cell invasion [28]. Our data suggest that integrin β 1 may directly regulate HIF-2 α expression, providing novel insight into this HIF pathway. However, the mechanism how integrin β 1 regulates HIF-2 α needs further investigation.

Conclusion

Taken together, our study demonstrates that HPA over-expression in MSCs contributes to augmented angiogenesis primarily through enhanced endothelial cell migration that is independent of the release of sequestered cytokines. We provide evidence that the mechanism involves activation of an integrin β 1/HIF-2 α /Flk-1/P38/HSP27 signaling pathway. The work provides new mechanistic insight into MSC therapy and places HPA as a key element that drives angiogenesis in this pathway. The results identify HPA as a means to augment therapeutic angiogenesis by MSCs either directly through gene insertion or by HPC.

Supplementary Material

Refer to Web version on PubMed Central for supplementary material.

Acknowledgments

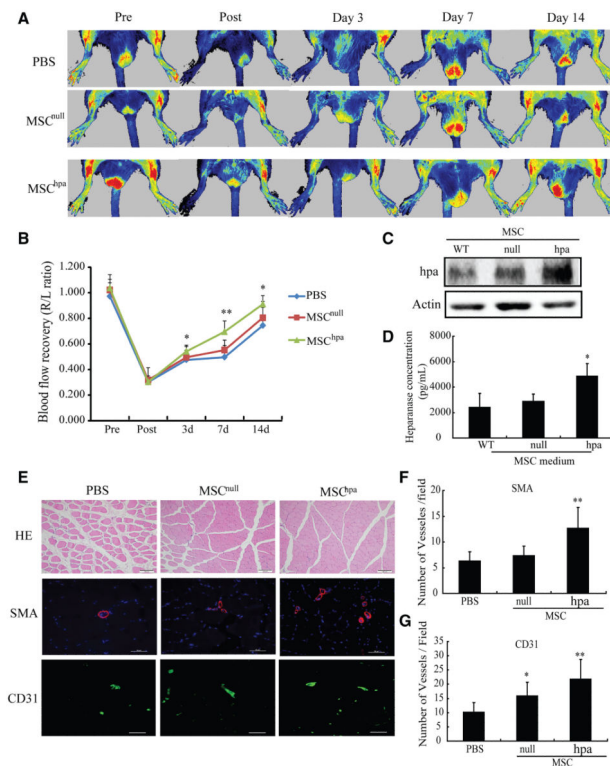
This work was supported by grants from National Natural Science Foundation of China (No. 31171418, 81320108003, 31371498 for J.W., No. 81170308, 81370247 for X.Y.H., No. 81202948 for L.Z., No. 81100141 for J.J.), National High-tech R&D 863 Program (No. 2013AA020101), The National Basic Research Program of China (973 Program, No. 2014CB965100, 2014CB965103), Science and Technology Department of Zhejiang province public welfare projects (No. 2013C37054), Zhejiang province key science and technology innovation team (No. 2010R50047), Major science and technology projects of Zhejiang province (2012C13013-3), The Fundamental Research Funds of Zhejiang University (No. 2012FZA7008 for L.D.), NIH Grant No. HL072924 (KAW), and by a Walter G. Ross Distinguished Chair in vascular biology (K.A.W.).

References

1. Heil M, Schaper W. Insights into pathways of arteriogenesis. *Curr Pharm Biotechnol.* 2007; 8:35–42. [PubMed: 17311551]
2. Koneru S, Varma Penumathsa S, Thirunavukkarasu M, et al. Sildenafil-mediated neovascularization and protection against myocardial ischaemia reperfusion injury in rats: Role of VEGF/angiopoietin-1. *J Cell Mol Med.* 2008; 12:2651–2664. [PubMed: 18373738]
3. Liang H, Hou H, Yi W, et al. Increased expression of pigment epithelium-derived factor in aged mesenchymal stem cells impairs their therapeutic efficacy for attenuating myocardial infarction injury. *Eur Heart J.* 2013; 34:1681–1690. [PubMed: 21606086]
4. Poitevin S, Cussac D, Leroyer AS, et al. Sphingosine kinase 1 expressed by endothelial colony-forming cells has a critical role in their revascularization activity. *Cardiovasc Res.* 2014; 103:121–130. [PubMed: 24743591]
5. Chamberlain G, Fox J, Ashton B, et al. Concise review: Mesenchymal stem cells: Their phenotype, differentiation capacity, immunological features, and potential for homing. *Stem Cells.* 2007; 25:2739–2749. [PubMed: 17656645]
6. Pisano C, Vlodyavsky I, Ilan N, et al. The potential of heparanase as a therapeutic target in cancer. *Biochem Pharmacol.* 2014; 89:12–19. [PubMed: 24565907]
7. Lever R, Rose MJ, McKenzie EA, et al. Heparanase induces inflammatory cell recruitment in vivo by promoting adhesion to vascular endothelium. *Am J Physiol Cell Physiol.* 2014; 306:C1184–1190. [PubMed: 24740543]
8. Fux L, Ilan N, Sanderson RD, et al. Heparanase: Busy at the cell surface. *Trends Biochem Sci.* 2009; 34:511–519. [PubMed: 19733083]
9. Purushothaman A, Hurst DR, Pisano C, et al. Heparanase-mediated loss of nuclear syndecan-1 enhances histone acetyltransferase (HAT) activity to promote expression of genes that drive an aggressive tumor phenotype. *J Biol Chem.* 2011; 286:30377–30383. [PubMed: 21757697]
10. Gingis-Velitski S, Zetser A, Flugelman MY, et al. Heparanase induces endothelial cell migration via protein kinase B/Akt activation. *J Biol Chem.* 2004; 279:23536–23541. [PubMed: 15044433]
11. Zetser A, Bashenko Y, Edovitsky E, et al. Heparanase induces vascular endothelial growth factor expression: Correlation with p38 phosphorylation levels and Src activation. *Cancer Res.* 2006; 66:1455–1463. [PubMed: 16452201]
12. Hu X, Yu SP, Fraser JL, et al. Transplantation of Hypoxia-preconditioned mesenchymal stem cells improves infarcted heart function via enhanced survival of implanted cells and angiogenesis. *J Thorac Cardiovasc Surg.* 2008; 135:799–808. [PubMed: 18374759]
13. Uemura R, Xu M, Ahmad N. Bone marrow stem cells prevent left ventricular remodeling of ischemic heart through paracrine signaling. *Circ Res.* 2006; 98:1414–1421. [PubMed: 16690882]
14. Chen HQ, Liu XB, Zhu W, et al. SIRT1 ameliorates age-related senescence of mesenchymal stem cells via modulating telomere shelterin. *Front Aging Neurosci.* 2014; 6:103. [PubMed: 24917814]
15. Limbourg A, Korff T, Napp LC, et al. Evaluation of postnatal arteriogenesis and angiogenesis in a mouse model of hind-limb ischemia. *Nat Protoc.* 2009; 4:1737–1746. [PubMed: 19893509]
16. Aicher A, Heeschen C, Sasaki K, et al. Low-energy shock wave for enhancing recruitment of endothelial progenitor cells: A new modality to increase efficacy of cell therapy in chronic hind limb ischemia. *Circulation.* 2006; 114:2823–2830. [PubMed: 17145991]

17. Redmond EM, Cahill PA, Hirsch M, et al. Effect of pulse pressure on vascular smooth muscle cell migration: The role of urokinase and matrix metalloproteinase. *Thromb Haemostasis*. 1999; 81:293–300.
18. Xu H, Czerwinski P, Hortmann M, et al. Protein kinase C α promotes angiogenic activity of human endothelial cells via induction of vascular endothelial growth factor. *Cardiovasc Res*. 2008; 78:349–355. [PubMed: 18056764]
19. Kim J, Kwak HJ, Cha JY, et al. The role of prolyl hydroxylase domain protein (PHD) during rosiglitazone-induced adipocyte differentiation. *J Biol Chem*. 2014; 289:2755–2764. [PubMed: 24338020]
20. Han Y, Yang K, Proweller A, et al. Inhibition of ARNT severely compromises endothelial cell viability and function in response to moderate hypoxia. *Angiogenesis*. 2012; 15:409–420. [PubMed: 22484908]
21. Kim HY, Yang DH, Shin SW, et al. CXXC5 is a transcriptional activator of Flk-1 and mediates bone morphogenic protein-induced endothelial cell differentiation and vessel formation. *FASEB J*. 2014; 28:615–626. [PubMed: 24136587]
22. Hedges JC, Dechert MA, Yamboliev IA, et al. A Role for p38MAPK/HSP27 pathway in smooth muscle cell migration. *J Biol Chem*. 1999; 274:24211–24219. [PubMed: 10446196]
23. Evans IM, Britton G, Zachary IC. Vascular endothelial growth factor induces heat shock protein (HSP) 27 serine 82 phosphorylation and endothelial tubulogenesis via protein kinase D and independent of p38 kinase. *Cell Signal*. 2008; 20:1375–1384. [PubMed: 18440775]
24. Wu S, Wu X, Zhu W, et al. Immunohisto-chemical study of the growth factors, aFGF, bFGF, PDGF-AB, VEGF-A and its receptor (Flk-1) during arteriogenesis. *Mol Cell Biochem*. 2010; 343:223–229. [PubMed: 20559689]
25. Scott A, Mellor H. VEGF receptor trafficking in angiogenesis. *Biochem Soc Trans*. 2009; 37:1184–1188. [PubMed: 19909243]
26. Fang HY, Hughes R, Murdoch C, et al. Hypoxia-inducible factors 1 and 2 are important transcriptional effectors in primary macrophages experiencing hypoxia. *Blood*. 2009; 114:844–859. [PubMed: 19454749]
27. Ridgway LD, Wetzel MD, Ngo JA, et al. heparanase-induced GEF-H1 signaling regulates the cytoskeletal dynamics of brain metastatic breast cancer cells. *Mol Cancer Res*. 2012; 10:689–702. [PubMed: 22513363]
28. Zetser A, Bashenko Y, Miao HQ, et al. Heparanase affects adhesive and tumorigenic potential of human glioma cells. *Cancer Res*. 2003; 63:7733–7741. [PubMed: 14633698]
29. Li Y, Liu H, Huang YY, et al. Suppression of endoplasmic reticulum stress-induced invasion and migration of breast cancer cells through the downregulation of heparanase. *Int J Mol Med*. 2013; 31:1234–1242. [PubMed: 23467544]
30. Liew A, O'Brien T. Therapeutic potential for mesenchymal stem cell transplantation in critical limb ischemia. *Stem Cell Res Ther*. 2012; 3:28. [PubMed: 22846185]
31. Roy M, Marchetti D. Cell surface heparan sulfate released by heparanase promotes melanoma cell migration and angiogenesis. *J Cell Biochem*. 2009; 106:200–209. [PubMed: 19115257]
32. Yamashita J, Itoh H, Hirashima M, et al. Flk1-positive cells derived from embryonic stem cells serve as vascular progenitors. *Nature*. 2000; 408:92–96. [PubMed: 11081514]
33. Wurmser AE, Nakashima K, Summers RG, et al. Cell fusion-independent differentiation of neural stem cells to the endothelial lineage. *Nature*. 2004; 430:350–356. [PubMed: 15254537]
34. Francescone R, Scully S, Bentley B, et al. Glioblastoma-derived tumor cells induce vasculogenic mimicry through Flk-1 protein activation. *J Biol Chem*. 2012; 287:24821–24831. [PubMed: 22654102]
35. Lee K, Qian DZ, Rey S, et al. Anthracycline chemotherapy inhibits HIF-1 transcriptional activity and tumor-induced mobilization of circulating angiogenic cells. *Proc Natl Acad Sci USA*. 2009; 106:2353–2358. [PubMed: 19168635]
36. Ben-Shoshan J, Schwartz S, Luboshits G, et al. constitutive expression of HIF-1 α and HIF2 α in bone marrow stromal cells differentially promotes their proangiogenic properties. *Stem Cells*. 2008; 26:2634–2643. [PubMed: 18687993]

37. Elvert G, Kappel A, Heidenreich R, et al. cooperative interaction of hypoxia-inducible factor-2 α and Ets-1 in the transcriptional activation of vascular endothelial growth factor receptor-2 (Flk-1). *J Biol Chem.* 2003; 278:7520–7530. [PubMed: 12464608]
38. Wada T, Shimba S, Tezuka M. transcriptional regulation of the hypoxia inducible factor-2alpha gene during adipose differentiation in 3T3-L1 cells. *Biol Pharm Bull.* 2006; 29:49–54. [PubMed: 16394508]
39. Chang LH, Pan SL, Lai CY, et al. Activated PAR-2 regulates pancreatic cancer progression through ILK/HIF- α -Induced TGF- α expression and MEK/VEGF-A-mediated angiogenesis. *Am J Pathol.* 2013; 183:566–575. [PubMed: 23764046]
40. Keely S, Glover LE, MacManus CF, et al. Selective induction of integrin beta1 by hypoxia-inducible factor: Implications for wound healing. *FASEB J.* 2009; 23:1338–1346. [PubMed: 19103643]

**Figure 1.**

MSC^{hpa} promotes vascular regeneration in vivo. **(A)**: Representative Laser-Doppler images (LDI) of hind limbs before, immediately after, and 3, 7, and 14 days after femoral artery occlusion. **(B)**: Quantitative LDI analysis showing the right-to-left (*R/L*) ratio; *n* for each group, * denotes *p* < .05. **(C)**: Detection of heparanase protein expression using Western blot in WT MSC, MSC harboring empty vector, and heparanase over-expressed vector. **(D)**: Detection of heparanase by ELISA in conditioned medium of WT MSC, MSC harboring empty vector, and heparanase over-expressed vector; *n* = 4 for each group, * denotes *p* < .05. **(E)**: HE and immunofluorescent staining of α -SMA and CD31 in muscle tissues from each group; Bar = 100 μ m for HE and Bar = 50 μ m for immunofluorescent staining. **(F, G)**: Bar graph showed quantitative analysis of SMA and CD31 positive area density; *n* = 5 for each group, * denotes *p* < .05; ** denotes *p* < .01. Abbreviations: MSC, mesenchymal stem cell; PBS, phosphate buffer saline; SMA, smooth muscle actin.

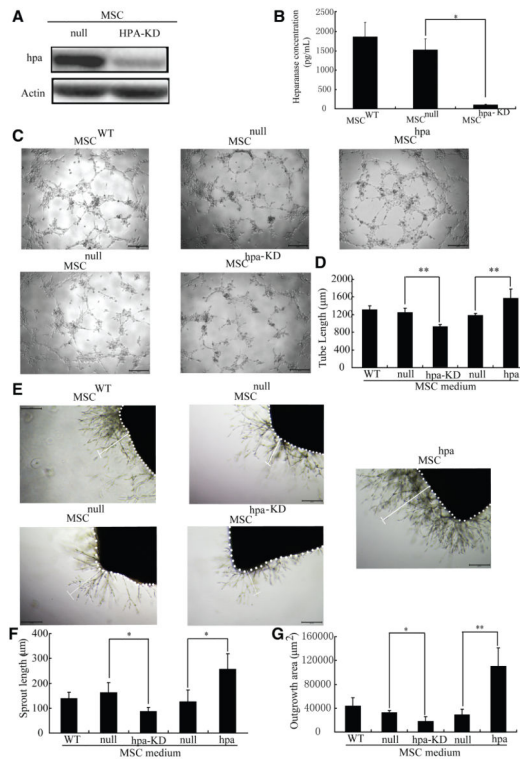


Figure 2. Proangiogenic role of MSC^{hpa} in vitro. **(A)**: Protein expression of heparanase and actin by Western blot in MSC^{null} and MSC^{hpa-KD}. **(B)**: Detection of heparanase concentration using ELISA in conditioned medium of MSC^{WT}, MSC^{null}, and MSC^{hpa-KD}; $n = 4$ for each group, * denotes $p < .05$. **(C)**: Representative images showing tube formation of human umbilical vein endothelial cells after cocultured with conditioned medium derived from MSC^{WT}, MSC^{null}, MSC^{hpa}, MSC^{hpa-KD}, respectively; Bar = 50 μm . **(D)**: Quantification of tube length in each group; $n = 3$ for each group, ** denotes $p < .01$. **(E)**: Aortic ring assay showing sprouting and branching in each group; Bar = 50 μm . **(F, G)**: Bar graph showed quantitative analysis of sprout length and outgrowth area, respectively; $n = 3$ for each group, * denotes $p < .05$, ** denotes $p < .01$. Abbreviation: MSC, mesenchymal stem cell.

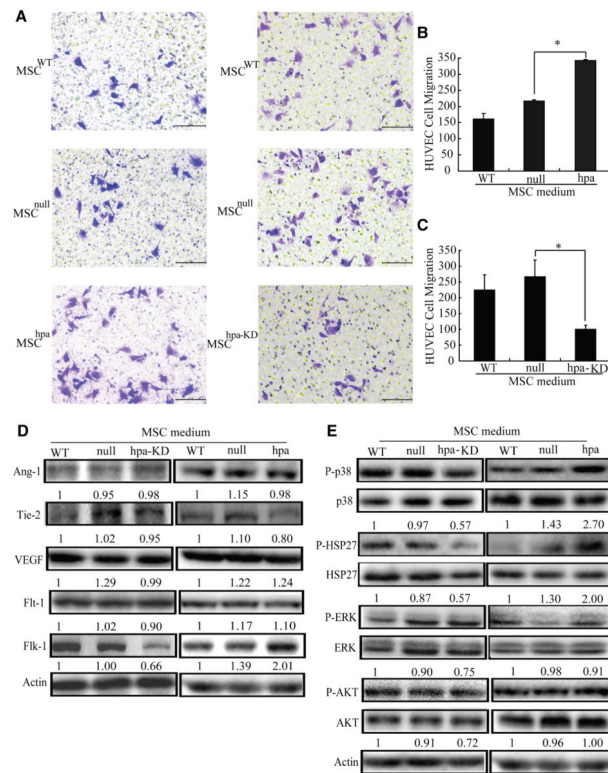


Figure 3. Enhanced cell migration by MSC^{hpa} via Flk-1/p38. **(A)**: Representative images showing cell migration of HUVECs after cocultured with conditioned medium derived from MSC^{WT} , MSC^{null} , MSC^{hpa} , MSC^{hpa-KD} , respectively; Bar = 50 μ m. **(B, C)**: Bar graph showing quantitative analysis of cell migration of HUVECs in each group; $n = 3$, * denotes $p < .05$. **(D, E)**: Quantification of VEGF, Flk-1, Flt-1, Ang1, Tie2, p-p38, p38, p-hsp27, hsp27, p-ERK, ERK, P-AKT, AKT, and actin expression by Western blot in MSC^{WT} , MSC^{null} , MSC^{hpa} , MSC^{hpa-KD} , respectively; $n = 3$. Abbreviations: HUVEC, human umbilical vein endothelial cell; MSC, mesenchymal stem cell.

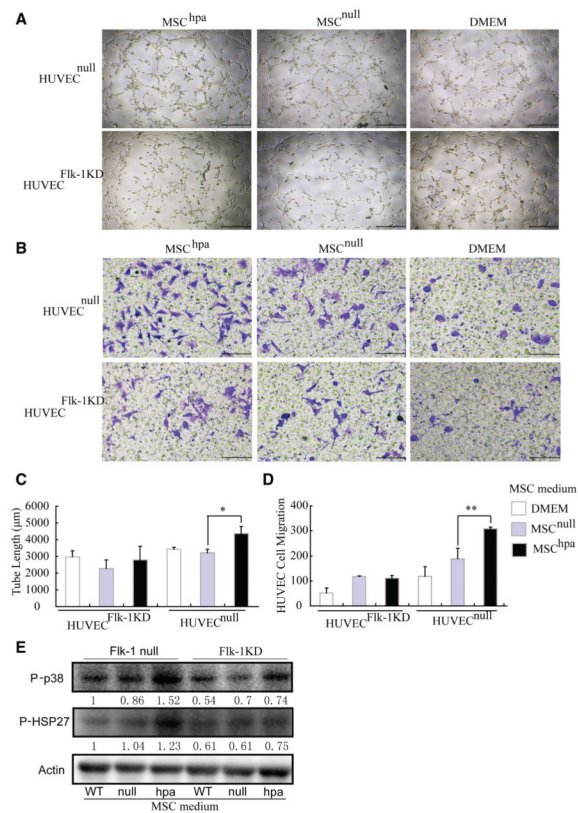


Figure 4.

Enhanced HUVEC migration and tube formation is mediated by Flk-1. (**A, B**):

Representative images showing cell migration and tube formation in HUVEC transfected with vector or Flk-1 shRNA lentivirus and cocultured with conditioned medium from MSC^{hpa}, MSC^{null}, DMEM; Bar = 100 μm for tube formation and Bar = 50 μm for migration.

(**C, D**): Bar graph showed quantitative analysis of tube length and cell migration,

respectively; $n = 3$ for each group, * denotes $p < .05$, ** denotes $p < .01$. (**E**): Western blot showing the expression of p-P38, p-hsp27 in HUVEC transfected with vector or Flk-1 shRNA lentivirus; $n = 3$. Abbreviations: HUVEC, human umbilical vein endothelial cell; MSC, mesenchymal stem cell.

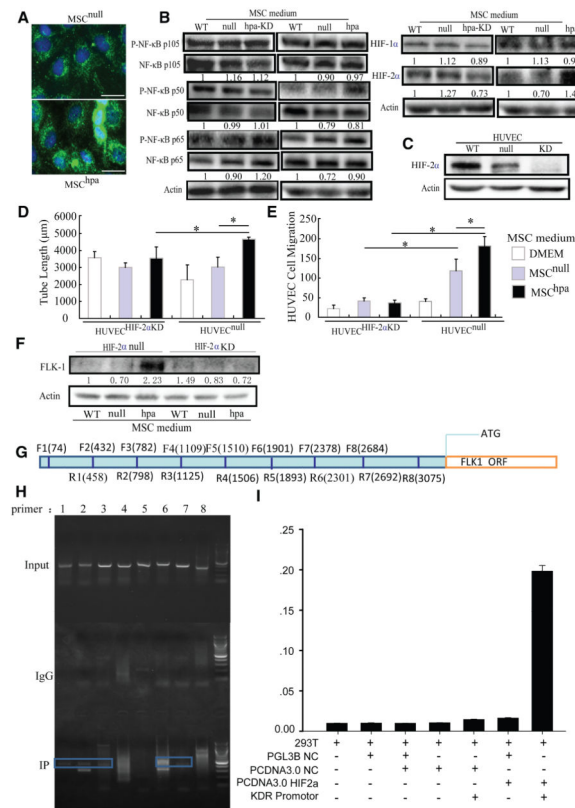


Figure 5. Activation of HIF-2 α and Flk-1 by MSC^{hpa}. **(A)**: Conditioned medium from MSC^{hpa} confers significantly increased nuclear accumulation of HIF-2 α in HUVECs, Bar = 25 μ m. **(B)**: Quantification of P-NF-KBp105, NF-KBp105, P-NF-KBp50, NF-KBp50, P-NF-KBp65, NF-KBp65, HIF-1 α , and HIF-2 α expression in HUVEC after coculture with conditioned medium from MSC^{null}, MSC^{hpa}, MSC^{hpa}-KD, respectively; $n = 3$. **(C)**: Quantification of HIF-2 α expression in HUVECs transfected with HIF-2 α shRNA by Western blot; $n = 3$ for each group. **(D, E)**: Bar graph showing quantitative analysis of tube length and cell migration, respectively; $n = 3$ for each group, * denotes $p < .05$. **(F)**: Western blot showing Flk-1 expression in HUVECs transfected with vector or HIF-2 α shRNA lentivirus cultured with conditioned medium from MSC^{wt}, MSC^{null}, and MSC^{hpa}; $n = 3$. **(G, H)**: Direct binding of HIF-2 α to the proximal promoter of Flk-1 confirmed by ChIP-PCR. **(I)**: Luciferase assay showing increased Flk-1 reporter activity by overexpression of HIF-2 α . Abbreviations: DMEM, Dulbecco's modified Eagle's medium; HUVEC, human umbilical vein endothelial cell; MSC, mesenchymal stem cell.

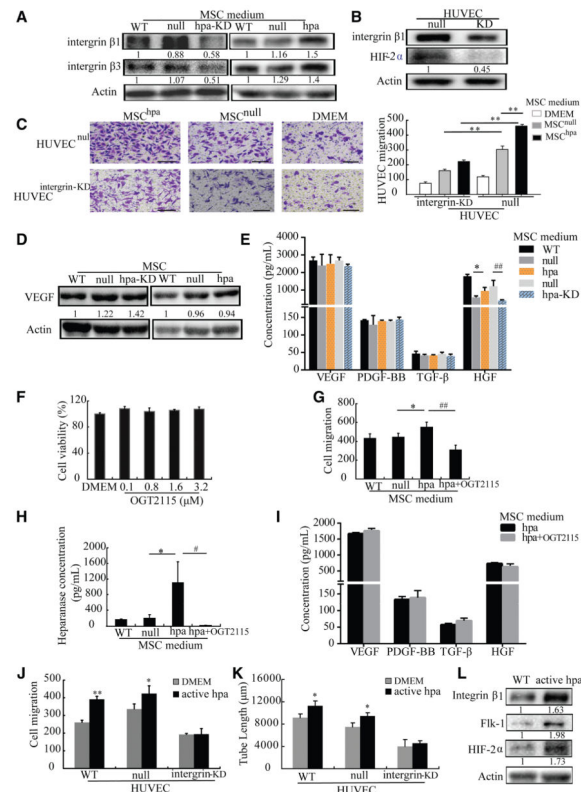


Figure 6. *HIF-2 α* activation by heparanase requires integrin $\beta 1$. (A): Western blot and quantification of integrin $\beta 1$ and $\beta 3$ expressions in HUVECs treated with conditioned medium from MSC^{null} , MSC^{hpa} , and MSC^{hpa-KD} . (B): *HIF-2 α* and integrin $\beta 1$ expressions are decreased in integrin $\beta 1$ knockdown HUVECs. (C): Representative images and bar graph of cell migration in HUVECs transfected with vector or integrin $\beta 1$ shRNA lentivirus; Bar = 50 μm , $n = 3$, ** denotes $p < .01$. (D): Quantification of VEGF expression in MSC^{WT} , MSC^{null} , MSC^{hpa-KD} , and MSC^{hpa} . (E): Quantification of VEGF, PDGF-BB, HGF, and TGF- β concentrations by ELISA in conditioned medium of MSC^{WT} , MSC^{null} , MSC^{hpa-KD} , and MSC^{hpa} , $n = 4$ for each group. * denotes $p < .05$ (hpa vs. null) and ### denotes $p < .01$ (hpa-KD vs. null). (F): Viability of MSCs in different concentrations of OGT2115 by CCK-8 assay. (G): Bar graph shows quantitative analysis of cell migration, respectively; $n = 3$ for each group. * denotes $p < .05$ (hpa vs. null), ### denotes $p < .01$ (hpa+OGT2115 vs. hpa). (H): Detection of heparanase concentration by ELISA in conditioned medium of MSC^{WT} , MSC^{null} , MSC^{hpa} , and $MSC^{hpa} + OGT2115$; $n = 4$ for each group, * denotes $p < .05$ (hpa vs. null), # denotes $p < .05$ (hpa+OGT2115 vs. hpa). (I): Detection of VEGF, PDGF-BB, HGF, and TGF- β concentrations by ELISA in conditioned medium of MSC^{hpa} and MSC^{hpa} with OGT2115, $n = 4$ for each group. (J, K): Bar graph shows quantitative analysis of cell migration and tube formation in each group; $n = 3$, ** denotes $p < .01$, * denotes $p < .05$. (L): Quantification of integrin $\beta 1$, Flk-1, and *HIF-2 α* expression in HUVECs after incubated with active heparanase; $n = 3$. Abbreviations: DMEM, Dulbecco's modified Eagle's medium; HUVEC, human umbilical vein endothelial cell; MSC, mesenchymal stem cell.

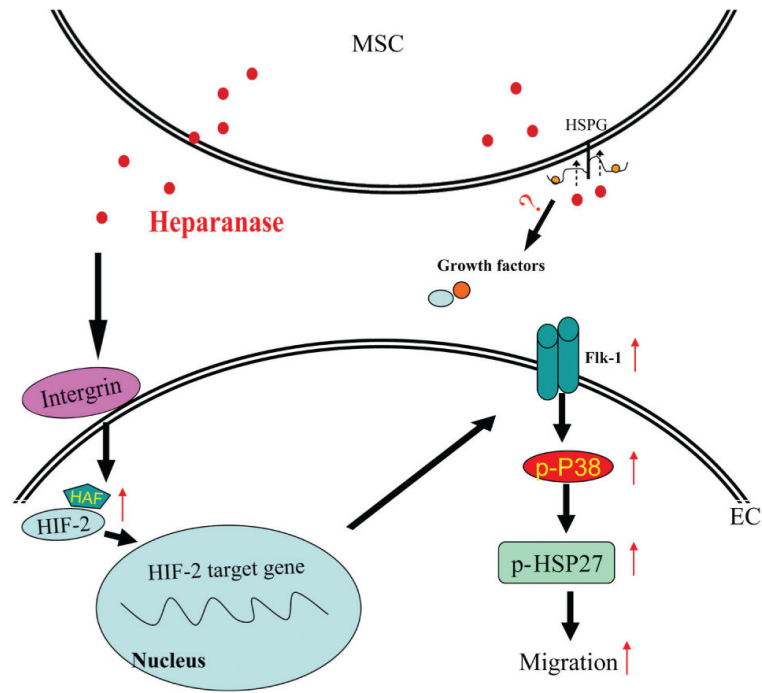


Figure 7. Schematic of cell migration and angiogenesis by MSC-secreted heparanase. Abbreviation: MSC, mesenchymal stem cell.